CORRECTING THE DIRECTION OF MOTION OF A DRONE BY ALTERING ITS CENTRE OF GRAVITY

Ariel Ang En Ren[1], Janika Oh Ja-Min[2], Yap Yong Keong[3]
[1]Victoria Junior College, 20 Marine Vista, Singapore 449035
[2]Raffles Institution (Year 5-6), 1 Raffles Institution Lane, Singapore 575954
[3]DSO National Laboratories, 12 Science Park Drive, Singapore 118225

---

1. Abstract

This project involves the altering of the centre of gravity (COG) of a drone to change its direction of motion. A stable flight is essential for accurate results during experimentation. Thus, a flywheel within the drone will be powered through an external motor before launch, allowing it to store rotational energy by its moment of inertia to keep the drone stable. In this study, a simple cylindrical body was used to remove secondary aerodynamic effects.

By 3D-printing these massive flywheels with different positions along the drone's centre rod, the COG of the drone can be altered. The PVC launcher will be angled downwards with the drone held in place. Upon release, the drone will slide down the pipe due, providing a component of the drone's horizontal velocity as it exits the pipe. After which, its landing position will be marked on an z-x plane to obtain a scatter plot.

Result analysis will determine the correlation between lateral forces on the drone and the position of its COG. If this theory holds true, changing a drone's direction of motion dynamically during flight by altering its centre of gravity using a set of motors would be feasible.

2. Background and Purpose of Research

Drones of all sizes contain propellers to control their direction of motion. Even the smallest drone, is made from a myriad of parts to enable its flight. Drones are limited by the reliability of its fragile propellers to provide lift, and if the propellers are damaged, the drone would not be able to fly.

Hence, the project focuses on the research of the feasibility of internal actuators within drones to adjust the flight path of a drone. With no external actuators like that of drones, the drone will be less fragile, such that during launch, there is no need to shield the actuators.

Through this research, the correlation between lateral forces on the drone and the position of its centre of gravity will determine if the implementation of internal actuators within a drone to alter its direction of motion during flight is feasible. This will increase the reliability of flight of a drone as there will be no external components that may compromise its flight.

3. Preliminary theory

The Magnus Effect was originally proposed to change the direction of the drone in the air. The Magnus Effect is the force exerted on a rapidly spinning cylinder or sphere moving through air or another fluid in a direction at an angle to the axis of spin. Notably, this effect is responsible for the swerving of balls when hit or thrown with spin[1].

However, vector diagrams revealed that during the flight of the drone in this project, the direction of the torque and the direction of air flow are parallel, resulting in no net force acting on the drone.

Torque-induced precession was thus proposed. Torque-induced precession, also known as gyroscopic precession is the phenomenon in which the axis of a spinning object, such as a gyroscope, describes a cone in space when an external torque is applied to it[2]. In this case, the two points that provide for this torque are the centre of pressure (COP) and the centre of gravity (COG). In the drone, the COP is fixed, while the COG changes. The COP is the point where the total sum of a pressure field acts on a body, causing a force to act through that point. For instance, if the COP is ahead of the COG, it produces a force towards the COG. If the object is spinning anti-clockwise from front view, this causes the object to move to its left. In theory, this, combined with the deflection of air around the drone, produces an external force on the drone, enabling it to change its direction in flight. This is similar to the rudder effect, where the displacement of the air causes a moment about the centre of gravity, causing the drone to turn mid-flight[3].

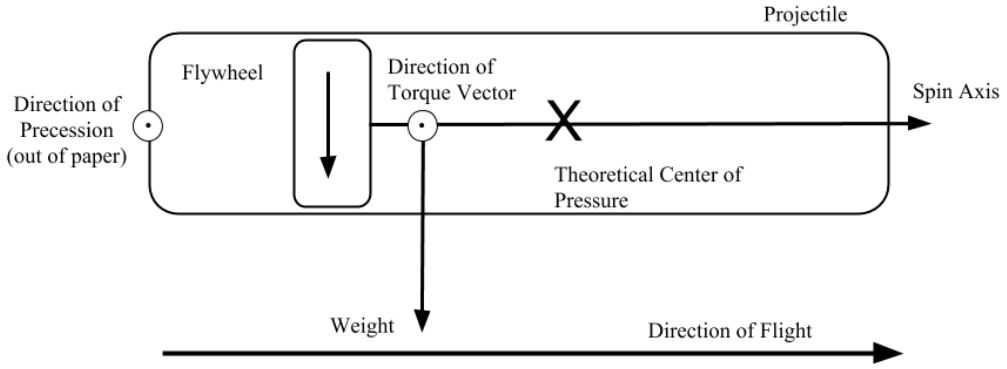

Figure 3.1 Diagram of Torque-Induced Precession

4. Design of Project Components

4.1 Drone

4.1.1 Conceptualisation of Internal Drone Design

A body is said to be stable if it can maintain a steady motion by developing moments or forces that allow it to restore itself to its original condition of equilibrium. For this drone, this is done by spinning the flywheel along its axis of symmetry. This produces stability in two ways.

Firstly, it will produce gyroscopic stability in the direction of motion as it creates angular momentum in the drone which is resistant to change. The conservation of angular momentum along the direction of flight reduces unwanted rotation or changes in flight path[4].

Secondly, air resistance is minimized, as the drone can cut through the air faster. Less energy is lost to creating turbulent air, allowing the drone to remain at a high speed for longer periods of time. Furthermore, the drone's flight path will also be straighter as there will be less air pressure acting on the body due to reduced turbulence[5].

Hence, to spin the drone during flight to ensure stability, it will contain a flywheel that will be externally powered by a motor. Upon launch, this flywheel would be able to continue spinning due to its stored rotational energy, providing for a moment of inertia that will resist changes in its rotational speed[6].

The flywheel consisted of a 3D-printed shell, with a mass made from hot glue and nuts to increase its weight (Annex A2). The hot glue mass weighed 265g, making up for more a third of the drone's entire mass. This was to ensure that any change in the flywheel's position will result in a very pronounced change in the drone's COG, making any deviation in flight path more noticeable. Coupled with the motor's max revolutions per minute (RPM) of approximately 20000, the flywheel will have a angular velocity of 728πrad/s (Annex B). More importantly, the projectile had a moment of inertia of $0.00074531 kgm^2$ (Annex C).

The initial idea was to create a drone where the position of flywheel could be remotely moved using internal actuators. Using lead screws and scissor linkages were considered. However, using such mechanisms to move the flywheel inside this small-scale drone would require numerous parts which could render the drone too heavy to launch or resulting in the launch distance being too short for any significant correlations to be identified. Next, it would make the change in COG by moving the flywheel to be less pronounced, resulting in difficulties in identifying a difference in results.

Therefore, it was concluded that an internal rod will hold a massive flywheel. Five configurations of this rod will be 3D-printed, with the position of flywheel changed to alter the drone's centre of gravity. With the length of drone being 20cm, the flywheels of height 4cm will be placed at 3cm intervals starting at 4.5cm from the rear of the drone, which is the outer edge of the rear bearing, to the middle of the flywheel. The position of the flywheels will thus be 4.5cm, 7.5cm, 10.5cm, 13.5cm and 16.5cm from the rear of the drone.

4.1.2 Drone Body Material

The materials considered for the drone body were polyethylene terephthalate (PET), polyvinyl chloride (PVC) and cardboard. Two factors were considered, namely density and tensile strength.

	Polyethylene Terephthalate (PET)	Polyvinyl Chloride (PVC)	Cardboard
Density / g cm^{-3}	1.39[7]	1.38[9]	0.69[10]
Tensile Strength / MPa	55[8]	2.6[9]	0.03[11]

Figure 4.1 Table of Comparison of Drone Body Material

Although the tensile strength of cardboard is significantly lower than the other two materials, cardboard was eventually chosen as the drone body material as it is lightweight. To make up for the lack of tensile strength, duct tape, which has a tensile strength of 22MPa[12], was wrapped around the cardboard tube to increase the drone's durability.

4.1.3 Final Drone Design

A drone of length 20cm was made from a 3-inch diameter cardboard roll with PVC pipe end caps of length, containing a 4cm-thick flywheel. A hole was drilled through each end cap to fit a bearing that would support the rod on which the flywheel would spin. The centre rod extended past the end caps to enable coupling with the motor to spin the flywheel. Washers and R-clips were used to secure the centre rod in place.

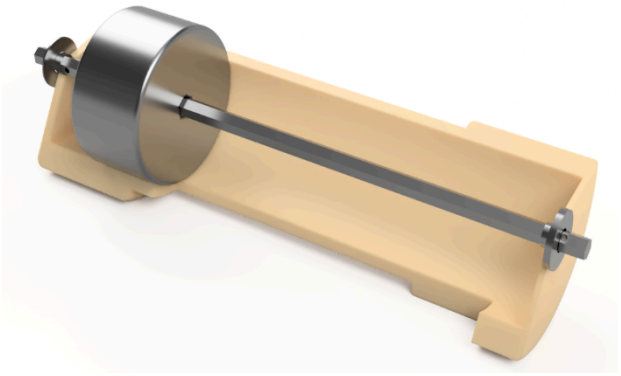

Figure 4.2 Cross-section Render of Drone

The rod and flywheel were designed in Autodesk Fusion 360 and were 3D-printed using Polylactic Acid (PLA). PLA has a high tensile strength of 26.4MPa, ensuring that it would not break during the impact of landing[13]. The centre rod was hexagonal to prevent the flywheel and rod assembly from slipping when the motor spins. Fillets were added to all edges of the 3D-printed parts to further increase its strength and durability by distributing stress over a broader area[14].

4.2 Launcher

4.2.1 Conceptualisation of Launcher Design

Two launcher designs were considered for the launching of the drone, which has a mass of 0.644kg, namely a vacuum cannon and sliding the drone down a pipe a distance above the ground. A vacuum cannon would involve creating burst discs using aluminium foil which would be secured over each end of the launcher using duct tape. A vacuum of 50kPa would be pulled, before the rear burst disc is punctured, allowing the surrounding air to rush in and propel the drone due to the difference in pressure. However, it was decided that using a vacuum cannon will be dangerous as the drone would have a minimum exit velocity of 29.5ms^{-1} (Annex D). The vacuum cannon would be unreliable and cumbersome due to using duct tape to secure each burst disc each launch, coupled with plausible leaks. Hence, the drone would be slid down a pipe instead.

4.2.2 Final Launcher Design

For the launcher, a 4-inch diameter PVC pipe of length 2m was used. A motor was mounted 5cm away from the rear end of the pipe, centered using two 3D-printed spindles (Fig. 4.3). Mounted 9.5cm in front of the spindle were L-shaped guides (Fig 4.4) to seat the drone in an adaptor that coupled the hexagonal centre rod to the motor armature for the flywheel to be externally rotated (Fig 4.5). A section of the top of the launcher was removed to enable securing and releasing of the drone.

Figure 4.3 Front Spindle (Left) and Back Spindle (Right) to Secure Motor

Figure 4.4 L-shaped Guides

Figure 4.5 Motor Adaptor

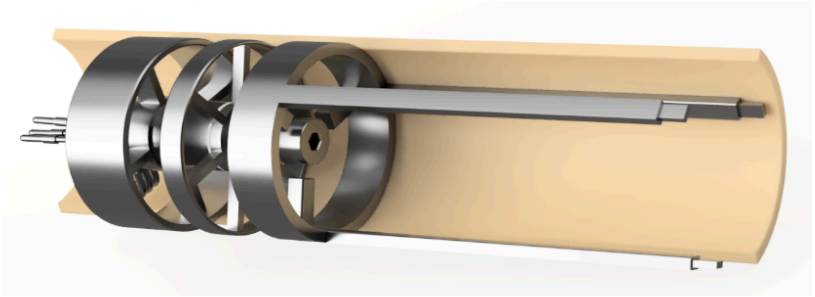

Figure 4.6 Cross-section Render of End of Launcher

4.3 Motor

The Racerstar 3660 2600Kv Brushless Motor was used as DC brushless motors are more efficient and produce more power and start-up torque as compared to brushed motors. An Austar Ax5s transmitter and companion receiver were used to control the motor speed. This system was powered by a fully-charged 2-cell lipo battery of 8.4v.

5. <u>Experimental Method</u>

The launcher was positioned at a 26.757^{o} angle below the horizontal and was aimed downwards to provide for the greatest theoretical horizontal range of 3.299m (Annex E). This was achieved by measuring the distance the drone would travel with respect to the centre of the drone, L_1, along with the height of the rail used to prop up the pipe, h_1.

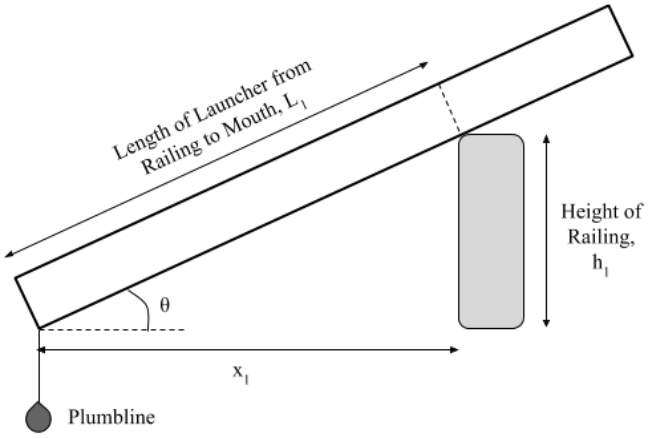

Figure 5.1 Diagram of Experimental Set-up

As $cos\theta = \frac{x_1}{L_1}$, $x_1 = L_1 \cos cos\, \theta$ and L_1 was determined to be half the length of the launcher at 1m. L_1 was marked on the launcher and a plumbline was attached to the mouth of the launcher. This plumbline was aligned to the origin of the x-z axis was marked on the ground, x_1 distance away from the railing on the first storey.

6. Results

Taking to the right and forward as positive,

Position of Flywheel / m	Distance Travelled in the z-axis / m	Distance Travelled in the x-axis / m	Angle of Motion / ◦
0.045	2.220	-0.050	1.29
0.075	2.565	-0.030	0.67
0.105	2.430	0.160	3.77
0.135	2.750	0.030	0.62
0.165	2.550	-0.500	11.1

Figure 6.1 Table of Results

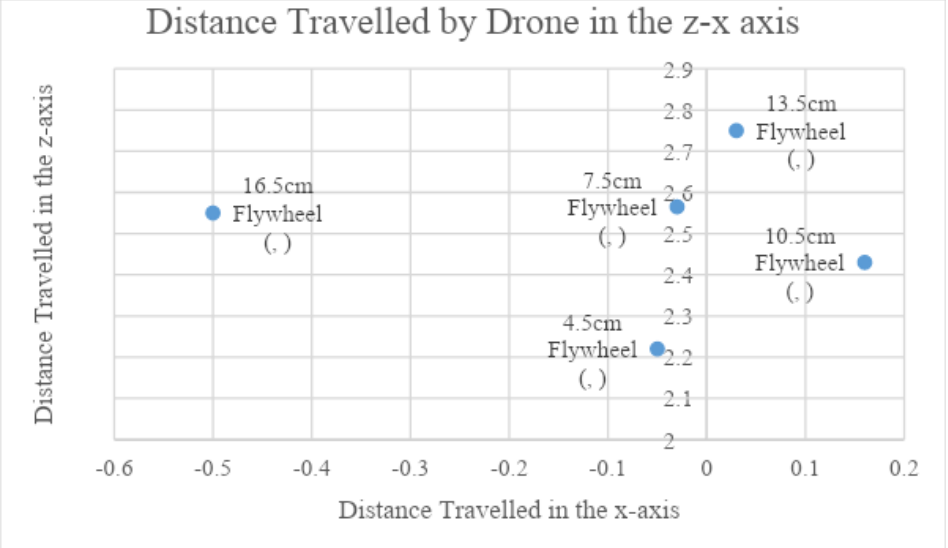

Figure 6.2 Scatterplot of Distance Travelled by Drone in the z-x axis

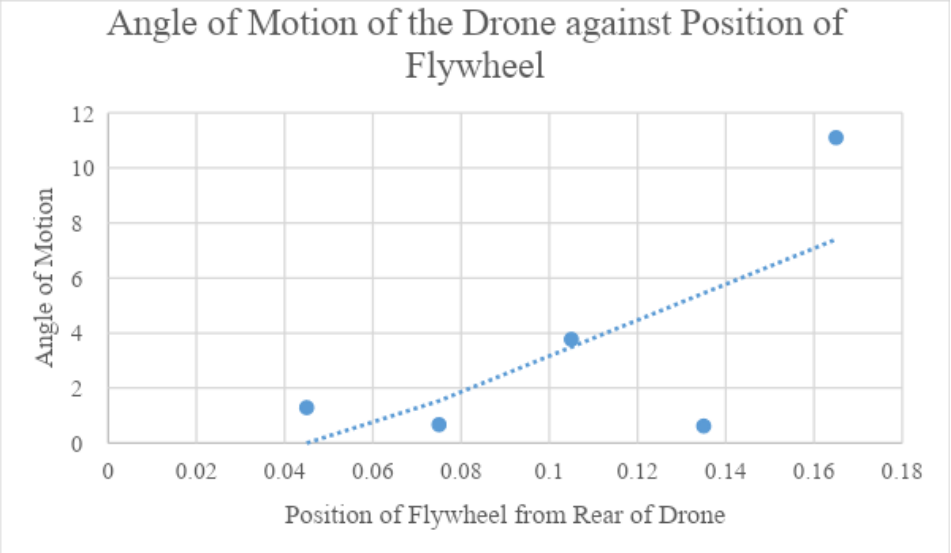

Figure 6.3 Scatterplot of Angle of Motion of the Drone against Position of Flywheel

7. Discussion

One problem faced during the experimentation was the choice of the material for the centre rod. Despite PLA's inherent strength, it was not able to withstand the torque produced by the brushless motor. This resulted in the rod being rounded down, preventing full transmission of the power of the motor to the flywheel. This would lead to inaccuracies during experimentation, as the final angular momentum of the projectile varies with each launch. More importantly, the PLA rods could not withstand the impact of the landings, resulting in them breaking after each launch. Hence, only one set of data could be obtained for each configuration of flywheel, which affected the reliability of results. Consequently, the if the flywheel adapter and flywheel rod could have been cut using a CNC router out of metal, this problem could have been eliminated.

Furthermore, the amount of energy dissipated as friction was difficult to estimate, as the area in contact between the drone and launcher was constantly changing. Compounded with the

fact that the launcher was 2m long, the amount of energy lost due to friction was larger than expected, hence making the calculations for the maximum horizontal range and angle of launcher inaccurate. A possible way to reduce the friction would be to lubricate the drone and the launcher.

As the final velocity of the drone was rather low of less than 3.97m/s, the rudder effect, which increases with airspeed[15] to cause a deflection in the flight path, was not noticeable, affecting the flight path only very slightly.

Due to the above issues, there was a lack of available data and a correlation between the position of flywheel in the drone and the direction of motion was undetermined. However, in future experiments, if the airspeed is increased, durability of the drone is improved, and the friction in the tube reduced, the hypothesis can be further refined.

8. Conclusion

A drone with a centre rod containing internal flywheels of different distances from the rear was developed. The rods and flywheels were 3D-printed using PLA and the body of the drone was made using cardboard wrapped with duct tape to increase tensile strength. The flywheels were located at 4.5cm, 7.5cm, 10.5cm, 13.5cm and 16.5cm from the rear of the drone. A launcher made from a 2m-long PVC pipe was also designed, with a brushless motor to externally power the flywheel before the drone is released.

However, due to problems faced during experimentation, only one reading was obtained per configuration of flywheel and hence, a correlation between the position of flywheel in the drone and the direction of motion was undetermined.

9. Acknowledgements

We would like to express our deepest appreciation to everyone who helped us with the project. We would like to thank Zheng Hong who helped us in our attempt to programme the ESC. We are also immensely grateful to Desmond, who was always eager to help us in the workshop be it with 3D-printing, providing us with materials that we needed or giving us advice on our prototypes. Last but not least, many thanks go to our project mentor, Yong Keong, for always checking in on us and providing valuable guidance and support in this project.

10. References

[1] Briggs, L. J. (1959). *Effect of Spin and Speed on the Lateral Deflection (Curve) of a Baseball ; and the Magnus Effect for Smooth Spheres*. Retrieved November 30, 2018, from https://web.archive.org/web/20110516150056/http://webusers.npl.illinois.edu/~a-nathan/pob/Briggs.pdf

[2] Boal, D. (2001). *Lecture 26 - Torque-free Rotation - Body-fixed Axes*. Retrieved December 4, 2018, from https://www.sfu.ca/~boal/211lecs/211lec26.pdf

[3] Chakraborty, S. (2017, October 9). How Does A Rudder Help In Turning A Ship? Retrieved December 5, 2018, from https://www.marineinsight.com/naval-architecture/rudder-ship-turning/

[4] Cali, D. (2013, October 1). Bullet Stability. Retrieved December 4, 2018, from https://bisonballistics.com/articles/bullet-stability

[5] Woodford, C. (2018, September 3). Bullets and missiles. Retrieved December 4, 2018, from https://www.explainthatstuff.com/bullets.html

[6] Kumar, S., & Das, J. (2013). *Application and Use of Flywheel in Engineering: Overview,1*(2). Retrieved November 30, 2018, from http://www.iraj.in/journal/journal_file/journal_pdf/6-33-139038931085-90.pdf

[7] Polyethylene Terephthalate Polyester (PET, PETP) - Properties and Applications - Supplier Data (2003, June 25). Retrieved December 6, 2018, from https://www.azom.com/article.aspx?ArticleID=2047

[8] Tensile Property Testing of Plastics (n.d.). Retrieved December 6, 2018, from http://www.matweb.com/reference/tensilestrength.aspx

[9] Polyvinyl Chloride PVC. (n.d.). Retrieved December 7, 2018, from http://www.bpf.co.uk/pvc-and-additives.aspx

[10] *Investigation 1: Density of Materials*. (2016-2017). Retrieved December 7, 2018, from http://sitesmedia.s3.amazonaws.com/chem/files/2016/06/F2016DensityProcedure1.pdf

[11] International Standards - Paper and Cardboard. (n.d.). Retrieved December 7, 2018, from https://www.ametektest.com/learningzone/standards/international-testing-standards-for-paper-and-cardboard

[12] Duct Tape By Strength - Compare Tensile Strength. (n.d.). Retrieved December 8, 2018, from https://www.tapemonster.com/pages/strongest-duct-tape

[13] MaterialTDS-PLA_01. (n.d.). Retrieved December 8, 2018, from https://www.sd3d.com/wp-content/uploads/2017/06/MaterialTDS-PLA_01.pdf

[14] Kupiec, H. (2016, June 19). Chamfer or Fillet: It's More Than a Coin Toss. Retrieved December 11, 2018, from https://www.engineering.com/AdvancedManufacturing/ArticleID/12682/Chamfer-or-Fillet-Its-More-Than-a-Coin-Toss.aspx

[15] Rudder. (2017, August 2). Retrieved December 12, 2018, from https://www.skybrary.aero/index.php/Rudder

11. Annexes

Annex A: Pictures of Components

Item	Picture
A1: Flywheel with Centre Rod (4.5cm from Rear)	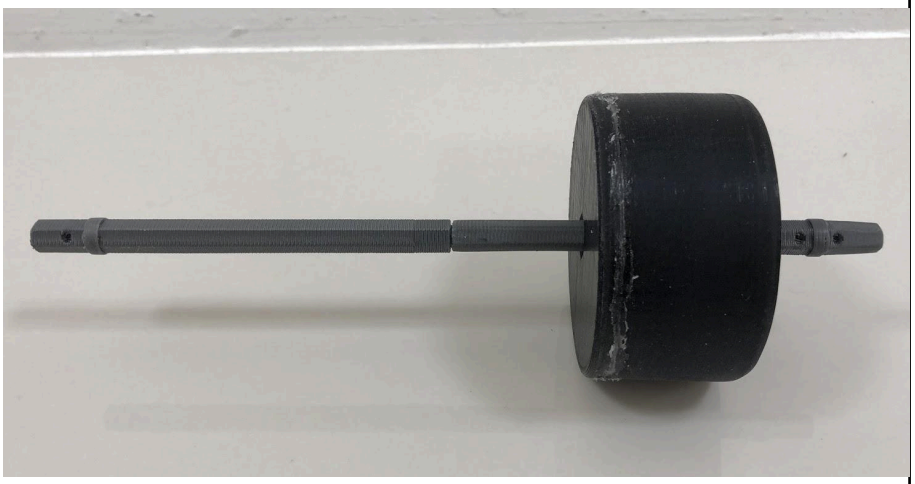
A2: Flywheel Mass Made of Hot Glue and Nuts	

A3: Drone Body	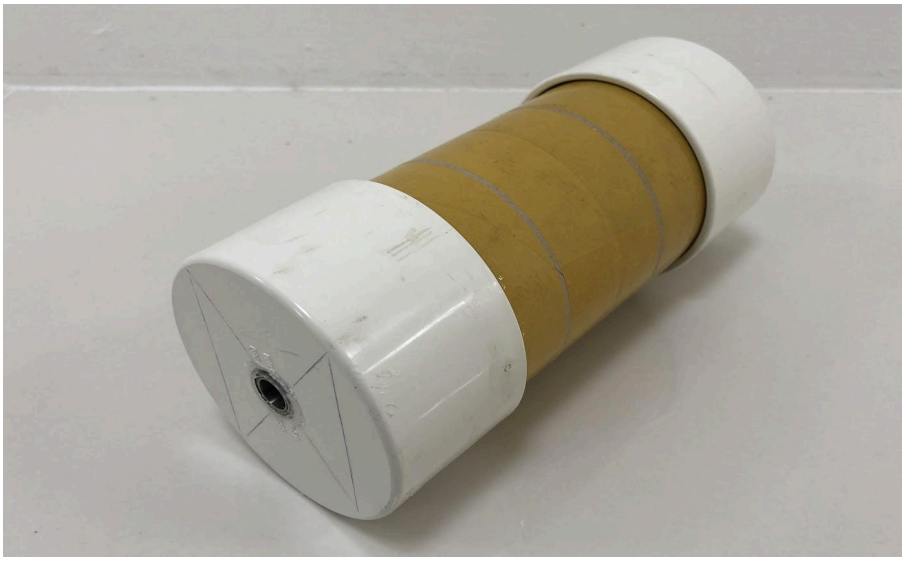
A4: Racerstar 3660 2600Kv Brushless Motor	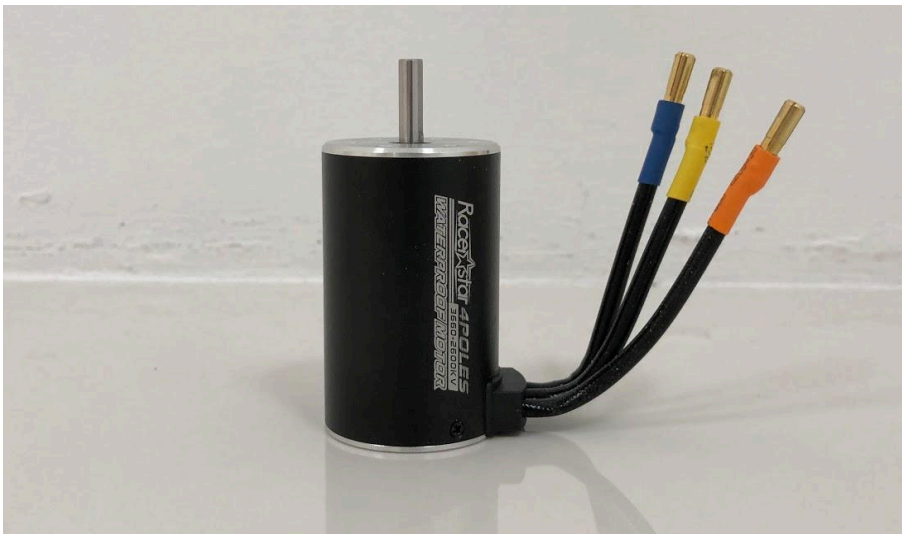
A5: Front (Left) and Back (Right) Spindle	

A6: Motor Adaptor	
A7: Assembled Motor, Spindles and Adaptor	
A8: Rear of Launcher	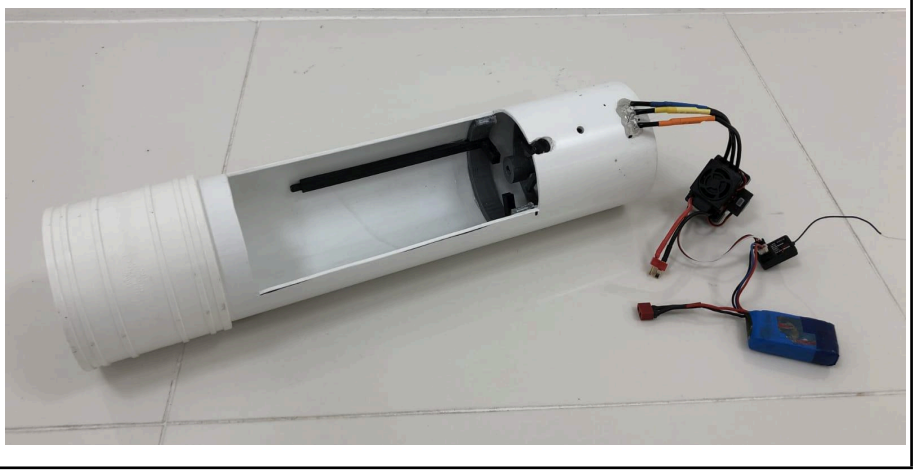

A9: Austar Ax5s Transmitter and Companion Receiver	

Annex B: Estimation of Maximum Revolutions Per Minute (RPM) of Flywheel

To find the maximum RPM of the motor,

$$Kv_{motor} \times Voltage_{motor} = RPM$$

As the motor's Kv is 2600 rpm per volt and the voltage across the motor is 8.4v,

$Maximum\ RPM = 21840rpm = 728\ \pi\ rad/s$, where $\frac{2\pi}{60} = 1\ rpm$

Annex C: Estimation of Moment of Inertia of Flywheel

For the moment of inertia, taking the flywheel as a solid cylinder,

$I = \frac{1}{2}MR^2 = 0.0007452kg\ m^2$, where R = 0.075m and M=0.265kg

Annex D: Estimation of the Maximum Velocity of a Drone Launched using a Vacuum Canon

As this a vacuum cannon could in theory launch a drone close to Mach speed, it was essential that realistic calculations of the maximum velocity of the drone in the context of our launcher was determined. This would involve assumptions of the 'worst case scenario', where values are rounded up and external forces such as friction are not included. This model also assumes that the drone's length is negligible, and that it is a perfect seal. Furthermore, the burst disc at the front of the launcher will not break.

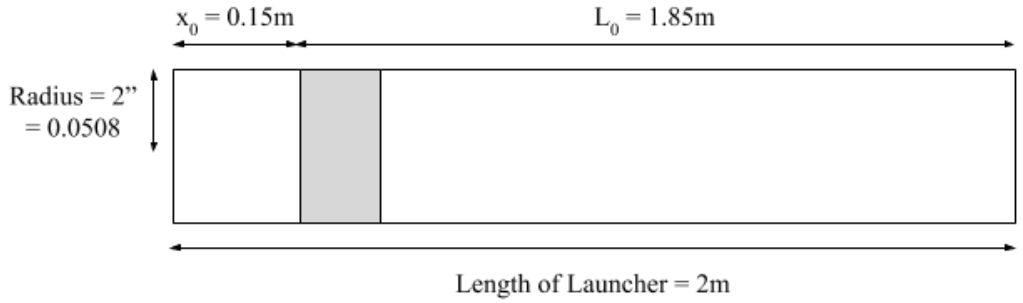

Figure 11.1 Diagram of Vacuum Canon

When pressure in L is equal to that of the pressure in x, air will stop rushing in. This will result in zero acceleration from this point onwards, labelled as y, which is the distance that x_0 increases while L_0 decreases until pressures in both sections are the same.

$$P_0V_0 = P_1V_1$$

For L, $P_vL_0A = P_{atm}\left(L_0 - y\right)A$, where P_v is the pressure inside the vacuum and A is the cross-sectional area of the launcher. Hence,

$$y = L_0(1 - \frac{P_v}{P_{atm}})$$

$$\text{Thus, } x_1 = x_0 + y \text{ and } L_1 = L_0 - y$$

Assuming that $P_{atm} = 101325Pa$ and $P_v = 80000Pa$, based on Figure ___ above, $y \approx 0.38936m$. Hence, $x_1 = 0.53936m$ and $L_1 = 1.46064m$.

While number of moles in L_0 is equal to the number of moles in L_1 as the burst disc is assumed not to break, number of moles from x_0 to x_1 increases as air from the surroundings rush in.

By utilizing $PV = nRT$ where T is the room temperature, one can obtain the number of moles in the air column, where $n = \frac{PV}{RT}$.

$$n_{L_1} = n_{L_0} = \frac{P_vL_0A}{RT}$$

$$n_{x_0} = \frac{P_v x_0 A}{RT}$$

$$n_{x_1} = \frac{P_{atm} x_1 A}{RT}$$

For L, since nRT is a constant, work done by air in L is given by,

$$W_L = \Delta P \Delta V = \left(P_{atm} - P_v\right)[\left(L_1 - L_0\right)A]$$

For x, the number of moles of air increases, so the formula $W = P\Delta V$ cannot be used. Hence,

$$W_x = \left(n_{x_1} - n_{x_0}\right)RT$$

$$W_{net} = W_x + W_L$$

Assuming that $T = 30^oC = 303.15K$, $W_{net} = 278.467J$.

Since $W_{net} = KE_{projectile} = \frac{1}{2} m_{projectile} v^2_{projectile}$,

$$v_{projectile} = \sqrt{\frac{2W_{net}}{m_{projectile}}}$$

Assuming the worst-case scenario and that acceleration is zero at this point, the maximum velocity of the drone of mass 0.644kg will be 29.5ms^{-1}.

Annex E: Estimation of Angle of Launcher to Provide for Maximum Distance Travelled

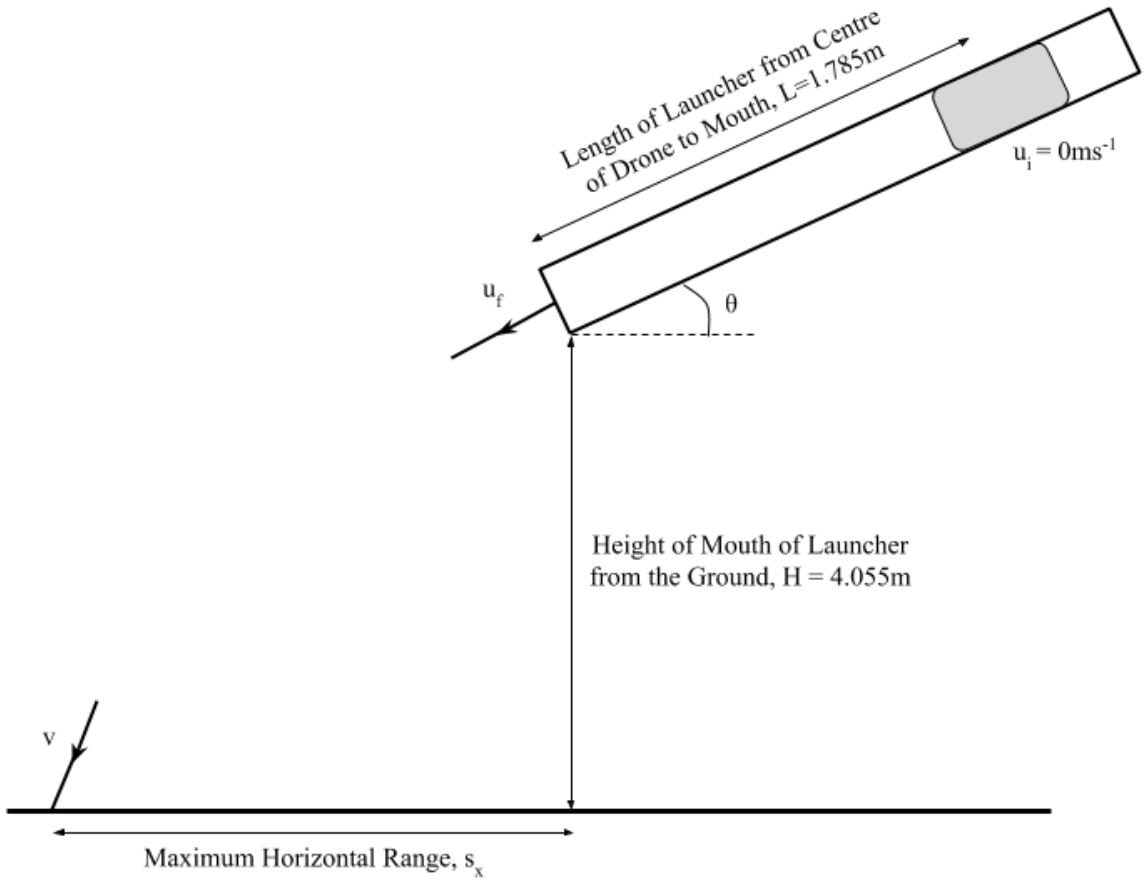

Figure 11.2 Diagram of Experimental Set-up for Calculations

In this project, the weight of drone is 0.644kg. Since $Loss\ of\ GPE = Gain\ in\ KE$, $mgLsin\theta = \frac{1}{2}mu_f^2$. Hence,

$$u_f = \sqrt{2gLsin\theta}$$

Therefore, $u_{f,x} = v_x = u_f cos\theta$ and $u_{f,y} = u_f sin\theta$.

By using the kinematics formula $s = ut + \frac{1}{2}at^2$, a quadratic equation of $\frac{1}{2}gt^2 + u_f \sin sin\,\theta\, t - H = 0$ can be obtained. The period of drone motion is obtained by,

$$t = \frac{-u_f sin\theta + \sqrt{u_f^2 sin^2\theta + 2gH}}{g}$$

Thereafter, an equation of the relationship between angle of launch and maximum horizontal range is obtained.

$$s_x = u_f \cos cos\,\theta\,(t) = -\sin sin\,2\theta\, L \sin sin\,\theta + 2\cos cos\,\theta \sqrt{L \sin sin\,\theta\,(Lsin^3\theta + H)}$$

By plotting a graph of

$s_x = -\sin sin\, 2\theta\, L \sin sin\, \theta + 2 \cos cos\, \theta \sqrt{L \sin sin\, \theta\, (Lsin^3\theta + H)}$, the maximum horizontal range that the drone would travel is 3.299m with a launch angle of 26.757° below the horizontal.